COMPUTATIONAL FLUID DYNAMICS SIMULATION OF HEAT TRANSFER PERFORMANCE OF EXHAUST GAS RE-CIRCULATION COOLERS FOR HEAVY-DUTY DIESEL ENGINES

by

Riad HADJAB [a*] ***and Mahfoud KADJA*** [b]

[a] Department of Drilling and Mechanic of Oil Yards,
University of Kasdi Merbah Ouragla, Algerie
[b] Laboratory of Applied Energetics and Pollution, Department of Mechanical Engineering,
University of Mentouri, Constantine, Algerie

Original scientific paper
https://doi.org/10.2298/TSCI160830317H

In order to estimate the performance of exhaust gas re-circulation coolers two factors were considered: the cooling efficiency and pressure drop. For that, three models of exhaust gas re-circulation coolers intended to heavy-duty Diesel engines were chosen and studied by numerical simulations. The CFD software FLUENT was used to solve the governing equations. Temperature dependant physical properties of the recycled exhaust gas were incorporated via the "User Defined Functions" feature of FLUENT. The inlet temperature of the exhaust gas is set to 523.15 K and the inlet mass-flow rate changes from 0.07 up to 0.2 kg/s. The computed performance results were compared to existing experimental measurements. The comparison of the computed results for the three models allowed to distinguish the exhaust gas re-circulation cooler model consisting of 19 tubes with helical baffles as having the best performance in terms of cooling efficiency and pressure drop.

Key words: *Diesel engine, NO_x, exhaust gas re-circulation cooler, cooling efficiency, FLUENT CFD*

Introduction

Emissions of NO_x and particulates are considered as the main problem of Diesel engines. High NO_x formation rates is the consequence of high temperature and high oxygen concentration [1]. Exhaust gas re-circulation (EGR) is among techniques that have proven a great performance in matters of reducing NO_x. Exhaust gases mainly consist of CO_2, water vapor, N_2, and O_2, which are more than 99% exhaust, while harmful pollutants are less than 1% of exhaust [2]. Once a part of this exhaust is redirected to the combustion chamber and dilute the intake charge, the proportion of O_2 will be reduced and consequently the combustion speed slows down. This also has the effect of rising the specific heat coefficient of the gas and thus reduce the peak cylinder temperature during combustion [3]. The EGR cooler is a heat exchanger which is incorporated in the system to reduce the recycled exhaust gas temperature required for the combustion chamber. This temperature is commonly comprised between 100 and 150 °C [4]. Many EGR cooler configurations are mentioned in the literature such as, shell and tube-type and stack-type [5]. Shell-and-tube type are present more than 35-40% of existing heat

* Corresponding author, e-mail: hadjab_riad@hotmail.com

exchangers for the reason of their robustness, easy maintenance and possible improvement [6]. The performance of the shell-and-tube type can be improved by helical baffles instead of segmental baffles. In fact, the use of helical baffles provides enhanced heat transfer performance, reduced pressure drop, less fouling in the shell side and lower costs [7]. Extensive experimental and numerical studies on EGR coolers were presented in the literature. Charnay *et al.* [4] carried out a numerical and experimental study on different EGR coolers in order to examine the influence of the shape of diffusers and the bundle size on results. Reynolds stress turbulence model was employed in their numerical simulation. However, the water side have not been included in their simulations assuming that the wall surface temperature of tubes as to be constant due to the high coolant flow. Huang *et al.* [8] presented numerical simulations of different EGR coolers with and without helical baffles and investigated their heat exchange performance. Moreover, they observed the impact of the entry directions of cooling water in EGR coolers with helical baffle on the flow resistance. Park *et al.* [9] investigated the influence of the internal shape of the EGR coolers with plain and spiral shaped tubes on heat exchange efficiency. They performed engine dynamometer experiments and numerical simulations using the commercial program FLUENT. It should be noted, from most studies, that physical properties of recycled exhaust gas which are dependent on temperature through the EGR cooler were not clearly defined. In the present paper, three models of EGR cooler, designed of multiple tubes and using water as coolant, are presented. Numerical simulations based on finite volume method are used to investigate the heat exchange performance of the EGR cooler. Detailed physical properties of the recycled exhaust gas constituents are associated to resolve the momentum, energy, and turbulence equations.

Mesh generation

Three models of the EGR cooler intended to heavy-duty Diesel engines are considered as shown in fig. 1. The first model (A) is an ordinary shell and tube type, made of 19 tubes with 10 mm diameter, the second model (B) is made with 61 tubes with 6 mm diameter, and the third one, model (c), is an improved model (A) by putting helical baffles on the shell side with baffle

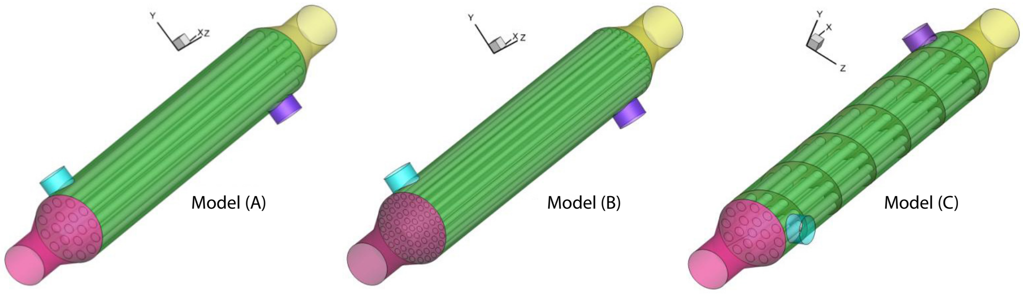

Figure 1. The EGR coolers geometry

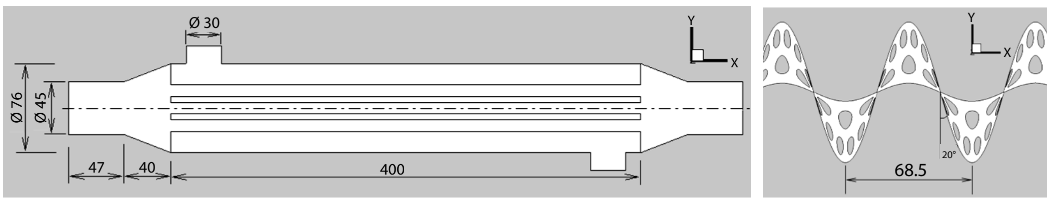

Figure 2. The EGR coolers dimensions; (a) diffusers and shell side dimensions, (b) baffle pitch and inclination angle

inclination angle α = 20° as presented in fig. 2. The three models share the same dimensions of diffusers, inlet and outlet of shell side as shown in fig. 2. Thickness of tubes and baffles are 0.6 mm. The middle line path of the water in the helical baffle is about 2.3 times than the water path without the baffle as are presented in tab. 1. Approximate velocity of gas and water for each configuration of EGR cooler are also given in tab. 1 at mass-flow rates of 0.1 kg/s for exhaust gas and 0.5 kg/s for water.

Table 1. Approximate velocities, middle line path and mesh information for each model

Model	Hexahedral cells number	Size of smallest size	Tetrahedral cells number	Size of smallest size	Approximate velocity [ms^{-1}] on gas side	Approximate velocity [ms^{-1}] on waters side	Middle line path from the inlet to the outlet [mm]
(A)	1531305	0.1080518	7872076	0.00161138	55	0.3	416
(B)	7732543	0.0198094	15770730	0.00178219	45	0.3	416
(C)	1531305	0.1080518	8413473	0.00095994	55	0.8	946

In this study, hexahedral mesh was chosen for the discretization of the tubes for the reason that the gas-flow inside is the most important region in the heat exchange. In addition, a boundary-layer mesh was generated at the inner wall of tubes. The water side, inlet and outlet diffusers in all models are discretized with tetrahedral mesh which is commonly used for geometries having complex areas as shown in fig. 3. The mesh is generated with the software ICEM CFD. The smallest cells are located close to the tubes wall for the reason that a fine resolution mesh is needed to investigate the heat exchange at this region. The number of mesh cells are summarized in tab. 1. Computations were performed on a PC with Intel Core i7-4770K CPU, 3.50 GHZ and 32 Go memory. Each simulation took about 6 hours for models (A) and (C) and about 24 hours for model (B) to converge.

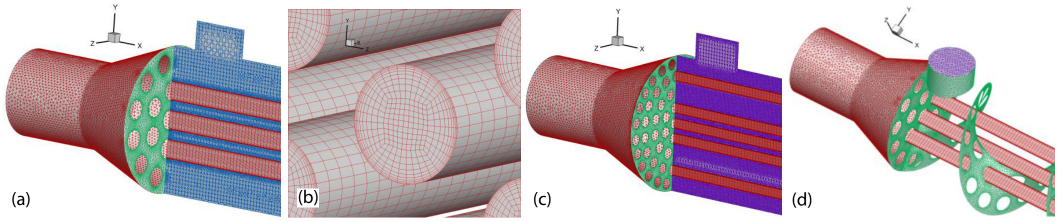

Figure 3. The EGR coolers grid; (a) computational grid of model (A), (b) computational grid of inner tubes, (c) computational grid of model (C), (d) computational grid of model (B)

Assumptions and boundary conditions

– No-slip boundary condition is applied on the walls of the shell and tubes surfaces within the computational domain. Standard wall function option is used for near-wall treatment [10].
– Mass-flow rate inlet boundary condition is affected to hot gas inlet for the range of 0.07 to 0.2 kg/s and inlet temperature of 523.15 K. Hot gas outlet was specified as a pressure outlet boundary condition.
– Cold fluid (water) enters the shell side through the inlet with constant mass-flow rate of 0.5 kg/s and temperature of 363.15 K, and leaves through the outlet with pressure outlet boundary condition.
– The shell wall of heat exchanger is set as adiabatic.

– The thickness of tubes wall and helical baffle are set to zero, since that inner and outer diameter are very close, which results that conduction resistance in solid region is negligible comparing to convection resistance for both sides.
– Coupled boundary condition is defined for energy transfer from the hot gas (inside the pipe) to the cold fluid (in the shell).
– The physical properties of the exhaust gas varied with temperature, however, the shell-side fluid (water) is assumed to be of constant thermal properties.
– The fluid-flow and heat transfer processes are turbulent and in steady-state.

Governing equations

In order to simulate the flow and heat transfer in the EGR cooler models, 3-D realizable *k*-turbulence models are applied [10]. The governing equations which are applied for both fluids can be expressed:

– *continuity equation*

$$\frac{\partial u_i}{\partial x_i} = 0 \tag{1}$$

– *momentum equation*

$$\frac{\partial u_i u_j}{\partial x_i} = -\frac{\partial P}{\rho \partial x_i} + \frac{\partial}{\partial x_j}\left[(\mu_t + \mu)\left(\frac{\partial u_j}{\partial x_i} + \frac{\partial u_i}{\partial x_j}\right)\right] \tag{2}$$

– *turbulent kinetic energy k-equation*

$$\frac{\partial \rho u_i k}{\partial x_i} = \frac{\partial}{\partial x_i}\left[\left(\mu + \frac{\mu_t}{\sigma_k}\right)\frac{\partial k}{\partial x_i}\right] + G_k - \rho\varepsilon \tag{3}$$

– *rate of energy dissipation equation*

$$\frac{\partial \rho u_i \varepsilon}{\partial x_i} = \frac{\partial}{\partial x_i}\left[\left(\mu + \frac{\mu_t}{\sigma_\varepsilon}\right)\frac{\partial \varepsilon}{\partial x_i}\right] + \rho C_1 S\varepsilon - \rho C_2 \frac{\varepsilon^2}{k + \sqrt{\nu\varepsilon}} \tag{4}$$

where G_k represents the generation of turbulence kinetic energy due to the mean velocity gradients and is given by:

$$G_k = -\rho\overline{u_i' u_j'}\frac{\partial u_i}{\partial x_j} = \mu_t S^2, \quad \mu_t = \rho C_\mu \frac{k^2}{\varepsilon} \tag{5}$$

$$C_1 = \max\left[0.43\frac{\eta}{\eta + S}\right], \quad \eta = S\frac{k}{\varepsilon}, \quad S = \sqrt{2S_{ij}S_{ij}}, \quad S_{ij} = \frac{1}{2}\left(\frac{\partial u_j}{\partial x_i} + \frac{\partial u_i}{\partial x_i}\right),$$
$$C_2 = 1.9, \quad \sigma_k = 1.0, \quad \sigma_\varepsilon = 1.2 \tag{6}$$

where S is the strain rate, μ_t – the turbulent viscosity, σ_k and σ_ε are the turbulent Prandtl numbers for k and ε.

– *energy equation*

$$\frac{\partial u_i T}{\partial x_i} = \rho\frac{\partial}{\partial x_i}\left[\left(\frac{\nu}{\mathrm{Pr}} + \frac{\nu_t}{\mathrm{Pr}_t}\right)\frac{\partial T}{\partial x_i}\right] \tag{7}$$

Physical properties of the exhaust gas

For modeling temperature dependent physical properties of the exhaust gas (which mainly consists of CO_2, water vapor, N_2, and O_2) such as density, viscosity, conductivity, and specific heat coefficient, we used respectively the following relationships:

$$\rho(T) = \frac{P_o}{\left[\left(\sum_i \frac{Y_i}{M_i}\right)\mathrm{R_{gas}}T\right]} \tag{8}$$

$$\mu(T) = \Sigma_i Y_i \cdot \mu_i \tag{9}$$

$$\lambda(T) = \Sigma_i Y_i \cdot \lambda_i \tag{10}$$

$$C_p(T) = \Sigma_i Y_i \cdot C_{pi} \tag{11}$$

The viscosity, conductivity and specific heat coefficient of each species i are given, respectively, by polynomial functions:

$$\mu_i = \sum_j a_{i,j} \cdot T^j, \quad k_i = \sum_j b_{i,j} \cdot T^j, \quad C_{pi} = \mathrm{R_{gas}} \cdot \sum_j c_{i,j} \cdot T^j \tag{12}$$

where the constants $a_{i,j}$ and $b_{i,j}$ are taken from Yaws' Transport Properties of Chemicals and Hydrocarbons [11] and the constants $c_{i,j}$ are taken from CHEMKIN thermodynamic database [12]. All these coefficients are in tab. 2.

Table 2. Coefficients for evaluation of physical properties of the exhaust gas

	j	0	1	2	3	4
CO_2		11.8109	0.49838	–1.0851E-04	0.0000E+00	0.0000E+00
		–1.2000E-02	1.0208E-04	–2.2403E-08	0.0000E+00	0.0000E + 00
		2.275724	0.009922072	–0.10409113E-04	0.06866686E-07	–0.02117280E-10
H_2O		22.8211	1.7387E-01	3.2465E-04	–1.4334E-07	0.0000E+00
		0.00561987	1.56992E-05	1.01063E-07	–2.42824E-11	0.0000E+00
		3.386842	0.003474982	-0.06354696E-04	0.06968581E-07	–0.02506588E-10
N_2		4.4656	0.63814	–2.6596E-04	5.4113E-08	0.0000E+00
		–0.000226779	0.000102746	–6.01514E-08	2.23319E-11	0.0000E+00
		3.298677	0.0014082404	–0.03963222E-04	0.05641515E-07	–0.02444854E-10
O_2		–4.9433	8.0673E-01	–4.0416E-04	1.0111E-07	0.0000E+00
		0.000154746	9.41534E-05	–2.75292E-08	5.20693E-12	0.0000E+00
		3.212936	0.0011274864	–0.05756150E-05	0.13138773E-08	–0.08768554E-11

Mass fractions calculations

In their research, Asad and Zheng [13] have proposed one-step global equations to calculate the transient and steady-state gas concentrations in the intake and exhaust. The equation given in the *Appendix A* represents the combustion reaction for steady-state EGR which is obtained by eliminating the cycle number from that which represents transient EGR and where is the effective EGR fraction that includes both the recirculated exhaust gas fraction and the in-cylinder combustion residual fraction [13].

Results and discussion

The computations are carried out using FLUENT, a commercial CFD code. The algorithm employed is SIMPLE. The second order up-wind scheme is used for the numerical simulation. The physical properties of the exhaust gas functions in eqs. (8)-(12) were programmed as User Defined Functions. Hybrid initialization is used for improving calculations robustness and making convergence faster comparing to standard initialization. Hybrid Initialization solves the Laplace equation to produce a velocity field that conforms to complex domain geometries, and a pressure field which smoothly connects high and low pressure values in the computational domain. All other variables (*i. e.* temperature, turbulence, *etc.*) will be patched based on domain averaged values [10].

Validation

The CFD simulations are validated by comparing computational results for model of 70 tubes studied in [4] with experimental ones. This validation is limited only to the gas side for mass-flow rates of 0.1 kg/s and 0.2 kg/s, assuming that the wall surface temperature of tubes may to be constant due to the high coolant flow [4] as previously mentioned. According to tab. 3, the pressure drop and the temperature results at the outlet show good agreement between computational and experimental ones.

Table 3. Pressure drop and temperature comparison of simulated and experimental results of 70 tubes model

Mass-flow rate [kgs^{-1}]	Simulated pressure drop [kPa]	Experimental pressure drop [kPa]	Simulated outlet temperature [K]	Experimental outlet temperature [K]
0.1	3.85	4.00	408.20	405.00
0.2	12.74	14.00	419.46	420.00

The CFD simulation of the gas side

Effect of the mass fraction of exhaust gas constituents on results

Although the R_{EGR} is mainly dependent on the mass-flow rate of recycled exhaust, this last is supposed constant when the R_{EGR} changes with the objective to examine the effect of the mass fractions of exhaust gas constituents on results. In the present work the diesel fuel $C_1H_{1.87}$ [13] and the excess-air ratio $\varphi_0 = 5$ are chosen, and according to previous relationships of eqs. (8)-(11), the mass fractions are calculated depending on the change of R_{EGR} and are presented in tab. 4.

Table 4. Mass fractions as functions of R_{EGR}

R_{EGR} [%]	$Y_{\mathrm{O_2}}$	$Y_{\mathrm{CO_2}}$	$Y_{\mathrm{H_2O}}$	$Y_{\mathrm{N_2}}$	$C_p(T_{g,i})$	$\mathrm{Pr}(T_{g,i})$	$T_{g,o}$ [K]
0	0.18395	0.04309	0.01648	0.75648	1059.55	0.71960	447.75
20	0.17187	0.05368	0.02053	0.75392	1063.90	0.72091	448.01
40	0.15192	0.07117	0.02722	0.74969	1071.05	0.72303	448.34
60	0.11267	0.10557	0.04038	0.74138	1085.14	0.72705	449.07
80	0	0.20434	0.07816	0.71750	1125.58	0.73730	451.14

It is found that as the mass fractions of the constituents change with the EGR ratio, the Prandtl number changes very slightly. Hence, the change of the exhaust gas constituents has slight effect on results. This can clearly be noticed from temperature values at the outlet of the EGR cooler which are calculated at constant mass-flow rate equal to 0.1 kg/s.

Pressure drop

The results in fig. 4 present the evolution of the pressure drop between the inlet and the outlet of the exhaust gas *vs.* inlet mass-flow rate of the recycled exhaust gas for the mod-

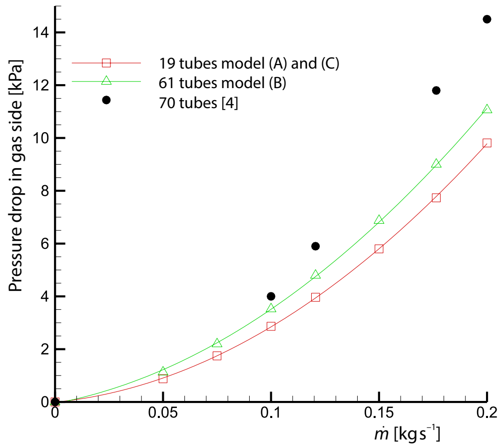

Figure 4. Pressure drop on gas side

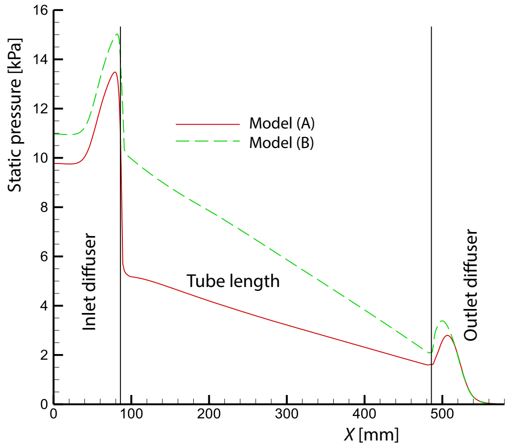

Figure 5. Static pressure along EGR coolers

els (A) and (B). Model (C) results are not presented here for the reason that gas side flows in model (A) and (C) are similar. These results are compared to the experimental results obtained by Charnay *et al*. [4], for an EGR cooler with 70 tubes of 6 mm of diameter. We can notice that the pressure drop increases as the number of tubes increases in the EGR cooler. Moreover, this increase becomes more important for high mass-flow rates. Figure 5 shows the evolution of the static pressure along the centerline of models (A) and (B), for an inlet mass-flow of 0.2 kg/s. It is clear that the conical shape of the inlet diffuser contributes in increasing the pressure, but the latter falls relatively just at the endplate. This drop in pressure in model (A) is greater than that in model (B). However, the inlet diffuser zone in model (A) shows that it is responsible for 47% of the overall pressure drop, while in model (B), it is responsible for only 9% of the overall pressure drop. On the other hand, the pressure drop proportion through the tubes zone is about 37% in model (A), while in model (B) is about 72%. In addition, the pressure drop over the tube length is given:

$$\Delta P = f\frac{L}{D_h}\rho\frac{U^2}{2} \tag{13}$$

where f is the friction factor, L and D_h are the length and the hydraulic diameter of the pipe, respectively, ρ – the density, and U – the mean velocity in the tube. From eq. (13), it is obvious that this difference in pressure drop is due not only to the number of tubes but also to the diameter of each model.

Cooling efficiency

The cooling efficiency, ξ, of a heat exchanger is principally defined as the actual heat transfer divided by the maximum possible heat transfer. For parallel flow heat exchangers, the cooling efficiency is calculated using the following expression [14]:

$$\xi = \frac{T_{g,i} - T_{g,o}}{T_{g,i} - T_{w,i}} \tag{14}$$

Figures 6 and 7 present, respectively, the change of efficiency and temperature with mass-flow rate, $\dot{m}$, of the recycled exhaust gas for all models including the experimental results of 70 tubes model [4]. Plots show that efficiency for model of 70 tubes is the highest, followed

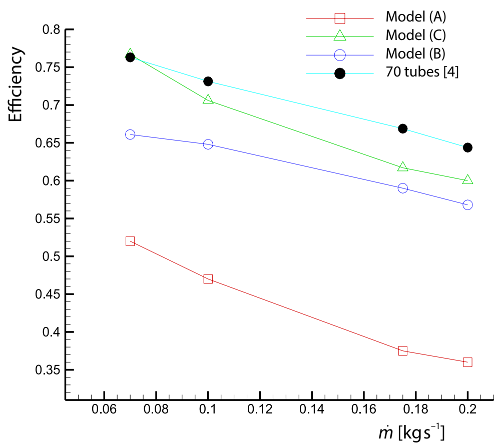

Figure 6. Cooling efficiency change

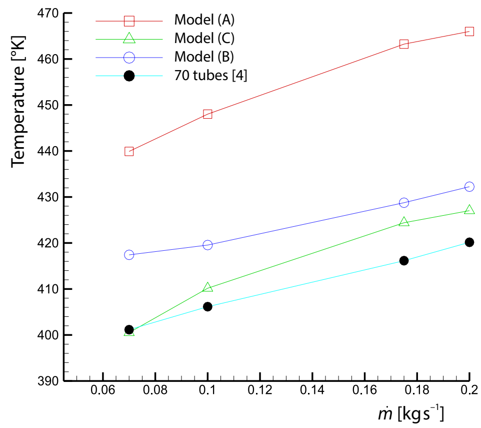

Figure 7. Temperature of exhaust gas at the outlet

by that of models (C) and (B) which provide better efficiency as compared to model (A). Actually, models (A), (B) and the model of 70 tubes [4] are all parallel flow heat exchangers types. The results therefore show that the more the number of tubes increases in these models, accordingly the heat transfer surface area becomes larger and the more the efficiency increases. Furthermore, for low mass-flow rates, model (C) is more efficient than model (B) and close to that in the model of 70 tubes. However, for high mass-flow rates, model (C) efficiency curve falls between the two. It can be said that model (C) possesses the characteristics of both cross and parallel flow heat exchangers types. This combination of flow types enhances the efficiency of the heat exchange by lengthening the flow path of the cooler.

Contours of temperature

In fig. 8 the contours of temperature are shown on longitudinal section views, for models (A), (B), and (C) at a mass-flow rate of 0.1 kg/s and with the same visualized method. From these contours, It is obvious that model (C) shows higher heat exchange comparing to other models. The reason that the helical path is longer enough to expand the heat transfer surface and therefore may compete the other models which use increased tubes bundle. It should be noted that EGR coolers have a limited volume due to the limited space under the vehicle head. Thus, helical baffle length will be increased by decreasing the inclination angle within the limits to not increasing pressure drop in the shell side. On the other hand, more compactness of EGR coolers could be obtained via decreasing tubes length at points where target temperatures are reached.

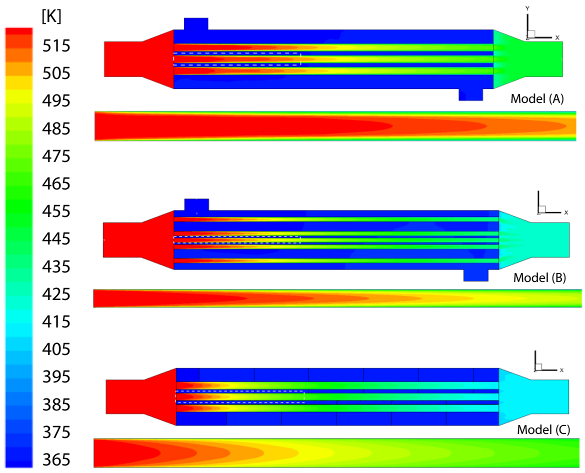

Figure 8. Contours of temperatures in tubes
(*for color image see journal web site*)

Contours of velocity magnitude

Contours of velocity magnitude and streamlines of the flow are shown in fig. 9 for model (A) and (B) at mass-flow rate of 0.1 kg/s. Furthermore, as it is mentioned previously, flows in models (A) and (C) are similar. It can be seen that the flow velocities are nearly uniform through the tubes of all models. It should also be noted that small recirculation regions with low velocity magnitude are located near conical wall and have no disturbance effect on the flow. These re-circulation regions is a consequence of the increase in diameter of the diffuser. Therefore, the diffuser is designed with adequate diameter at the inlet in order to avoid creating bigger recirculation regions which may preclude the flow particularly inside the outer crown of tubes bundle.

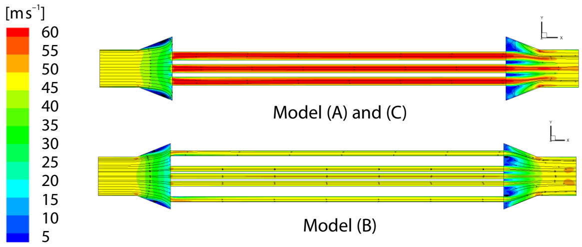

Figure 9. Contours of velocity magnitude in gas side (*for color image see journal web site*)

The CFD simulation of the water side

Pressure drop

The pressure drop between the inlet and the outlet of the shell side of all models against mass--flow rate are presented in fig. 10. Plots show that the difference of the pressure drop between models (A) and (C) is higher than that between models (A) and (B). In fact, the pressure drop values in model (B) are about 87% greater than those in model (A). However, in model (C) the values are about 1.34 times than those in model (A). Equation (13) reveals that two parameters clarify the difference in pressure drop between models (A) and (B). Firstly, the reduced hydraulic diameter, D_h, in model (B) as compared to that in model (A), given that, the hydraulic diameter of the water side of heat exchangers with n tubes, is defined by:

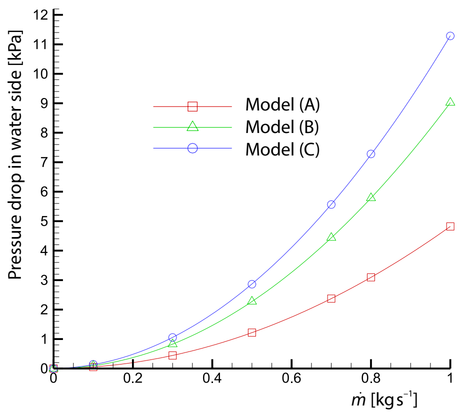

Figure 10. Pressure drop on water side for each model

$$D_h = \frac{2\left(R^2 - nr^2\right)}{R + nr} \tag{15}$$

where R is the shell outside radius, r – the tube radius, and n – the number of tubes [8]. Secondly, the average velocity, U, is higher in model (B) than that in model (A). On the other hand, the reason which explains the difference in values between models (A) and (C) is only one parameter which is the helicoidal length, L, traveled by the cooling fluid. Hence, as the helicoidal path increases the pressure drop increases. It should be noted that experimental results of the water side are not available regarding EGR cooler study of 70 tubes [4], for the reason that authors were focused in their study only on the gas side. However, from eqs. (13) and (15) and the results obtained previously, it is expected that the pressure drop through the water side of 70 tubes will increase. Indeed, as the number of tubes increases the hydraulic diameter of the shell side will decrease and simultaneously, the average velocity, U, increases and as a result, the pressure drop will increase.

Contours of temperature

Figure 11 shows the contours of temperature on perspective views, one can notice the change of the coolant temperature in the tubes vicinity and at the outlet of the shell side. The coolant temperature change is only a few degrees in all simulations, due to the high coolant flow of 0.5 kg/s. In fact, the temperature change calculated at the outlet of the shell side is of 3 °C for model (A), of 5 °C for model (B), and of 6 °C for model (C). On the other hand, the heat transfer balance relations for heat exchangers are expressed:

$$Q = (\dot{m}C_p)_{\mathrm{w}} \left(T_{\mathrm{w,o}} - T_{\mathrm{w,i}}\right) = (\dot{m}C_p)_{\mathrm{g}} \left(T_{\mathrm{g,i}} - T_{\mathrm{g,o}}\right) \tag{16}$$

Therefore, the outlet temperature of the water side is:

$$T_{\mathrm{w,o}} = \frac{(\dot{m}C_p)_{\mathrm{g}} \left(T_{\mathrm{g,i}} - T_{\mathrm{g,o}}\right)}{(\dot{m}C_p)_{\mathrm{w}}} + T_{\mathrm{w,i}} \tag{17}$$

Once calculations results are converged, the outlet temperatures of water side for each model are checked by means of the eq. (17), giving for this case: C_{p_w} = 4205J/kgK is specific heat coefficient of water for 363.15 K (taken from thermodynamic tables of water), $C_{p,g}$ = 1063.90 J/kgK is specific heat coefficient of exhaust gas which calculated from eq. (11) at 523.15 K, $\dot{m}_{\mathrm{w}}$ = 0.5 kg/s.

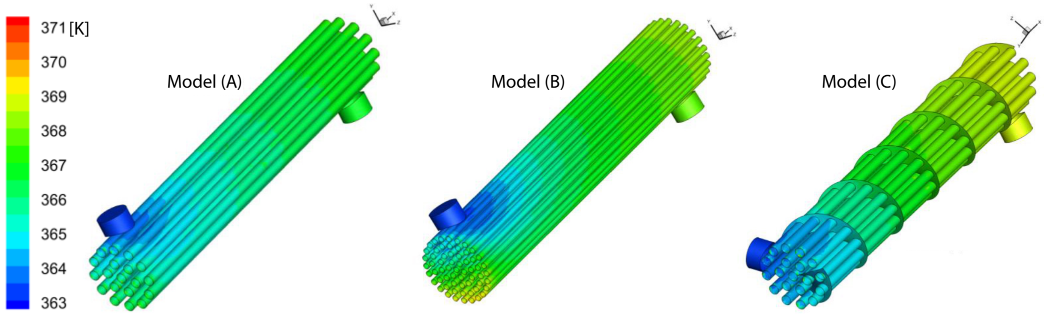

Figure 11. Contours of temperature on water side of tubes (*for color image see journal web site*)

Contours of velocity magnitude

Figure 12 shows, respectively, the contours of velocity magnitude on longitudinal and cross-section views of water side in models (A), (B), and (C) and at mass-flow rate of 0.5 kg/s. One can see from these figures that velocity magnitude increases just at the time the water attains the first tubes because of the reduced cross-section. On the other hand, these contours allow also to localize dead zones characterized by low velocities magnitude. In fact, the bottom of the inlet cross-section and the above of the outlet cross-section represent the zones that have the lowest velocity magnitude in both model (A) and (B). Moreover, near the inlet and the outlet of model (C), the corners situated between endplates and helical baffle have also lowest velocity magnitude. These dead zones have the effect of reducing heat transfer performance and increasing fouling problem. Therefore, given that mass-flow rates are not enough to get rid of these zones, some adjustments in geometry design should be taken into account. For instance, in order to reduce dead zones located in both corners of model (C), inlet and outlet cylinders with smaller diameter could be moved each one to its appropriate corner.

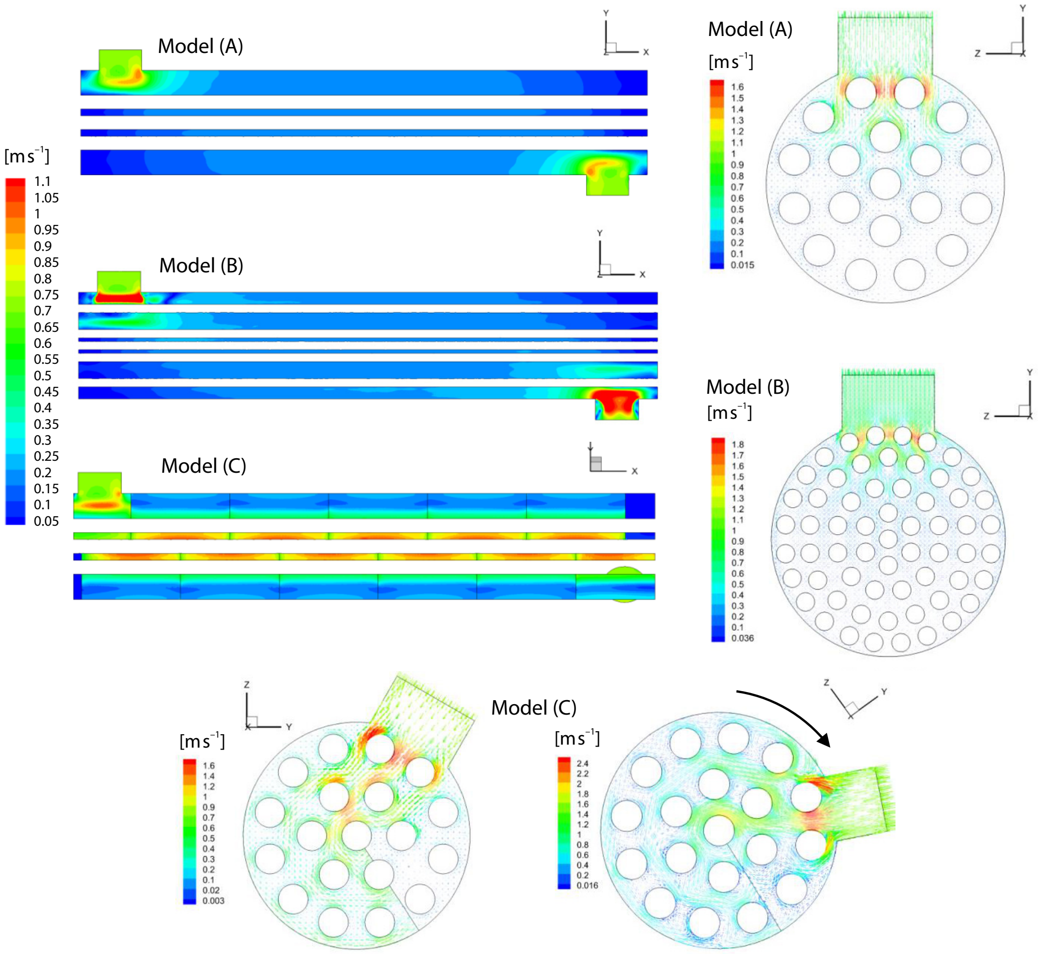

Figure 12. Contours of velocity magnitude on water side (m/s) (*for color image see journal web site*)

Conclusion

Performance of EGR coolers is estimated from many aspects. That is, size, cost, weight, cooling efficiency, pressure drop, and robustness. In the present study a CFD simulation on gas and water sides was performed for three models of EGR coolers. In order to estimate the performance of each model, two parameters such as cooling efficiency and pressure drop are considered. Firstly, it was found that the constituent mass fractions of the exhaust gas change with the EGR ratio has an insignificant effect on computational results. It was also shown, from results of EGR coolers of 61 tubes and of 70 tubes, that when the number of tubes increases the efficiency increases, however, the pressure drop increases too through gas and cooler sides. So a compromise between efficiency and pressure drop has to be achieved to optimize the system within the limits, as the case of the model (C) which exhibits better performance in terms of efficiency and pressure drop. Finally, it is shown that the coolant temperature changes by only a few degrees in all simulations, due to the high coolant flow. In addition, dead zones found on the water side could be avoided by making some changes in geometry design.

Appendix A

$$C_\alpha H_\beta C_\gamma + \varphi_0\left(\alpha+\frac{\beta}{4}-\frac{\gamma}{2}\right)3.76\mathrm{N_2} + \frac{R_\mathrm{EGR}}{1-R_\mathrm{EGR}}\left(\alpha\mathrm{CO_2}+\frac{\beta}{2}\mathrm{H_2O}\right)+\left(\alpha+\frac{\beta}{4}-\frac{\gamma}{2}\right)\left(\varphi_0-\frac{R_\mathrm{EGR}}{1-R_\mathrm{EGR}}\right)\mathrm{O_2}\rightarrow$$

$$\rightarrow\frac{1}{1-R_\mathrm{EGR}}\left(\alpha\mathrm{CO_2}+\frac{\beta}{2}\mathrm{H_2O}\right)+\left(\alpha+\frac{\beta}{4}-\frac{\gamma}{2}\right)\left[3.76\varphi_0\mathrm{N_2}+\left(\varphi_0-\frac{1}{1-R_\mathrm{EGR}}\right)\mathrm{O_2}\right] \qquad [13]$$

Mass fractions for exhaust gas species are given:

$$Y_{\mathrm{O_2(ex)}}=\frac{\left(\alpha+\frac{\beta}{4}-\frac{\gamma}{2}\right)\left(\varphi_0-\frac{1}{1-R_\mathrm{EGR}}\right)M_\mathrm{O_2}}{\left(\frac{1}{1-R_\mathrm{EGR}}\right)\left(\alpha M_\mathrm{CO_2}+\frac{\beta}{2}M_\mathrm{H_2O}\right)+\left(\alpha+\frac{\beta}{4}-\frac{\gamma}{2}\right)\left(3.76\varphi_0 M_\mathrm{N_2}+\left(\varphi_0-\frac{1}{1-R_\mathrm{EGR}}\right)M_\mathrm{O_2}\right)}$$

$$Y_{\mathrm{CO_2(ex)}}=\frac{\alpha\left(\frac{1}{1-R_\mathrm{EGR}}\right)M_\mathrm{CO_2}}{\left(\frac{1}{1-R_\mathrm{EGR}}\right)\left(\alpha M_\mathrm{CO_2}+\frac{\beta}{2}M_\mathrm{H_2O}\right)+\left(\alpha+\frac{\beta}{4}-\frac{\gamma}{2}\right)\left(3.76\varphi_0 M_\mathrm{N_2}+\left(\varphi_0-\frac{1}{1-R_\mathrm{EGR}}\right)M_\mathrm{O_2}\right)}$$

$$Y_{\mathrm{H_2O(ex)}}=\frac{\frac{\beta}{2}\left(\frac{1}{1-R_\mathrm{EGR}}\right)M_\mathrm{H_2O}}{\left(\frac{1}{1-R_\mathrm{EGR}}\right)\left(\alpha M_\mathrm{CO_2}+\frac{\beta}{2}M_\mathrm{H_2O}\right)+\left(\alpha+\frac{\beta}{4}-\frac{\gamma}{2}\right)\left(3.76\varphi_0 M_\mathrm{N_2}+\left(\varphi_0-\frac{1}{1-R_\mathrm{EGR}}\right)M_\mathrm{O_2}\right)}$$

$$Y_{\mathrm{N_2(ex)}}=\frac{3.76\varphi_0\left(\alpha+\frac{\beta}{4}-\frac{\gamma}{2}\right)M_\mathrm{N_2}}{\left(\frac{1}{1-R_\mathrm{EGR}}\right)\left(\alpha M_\mathrm{CO_2}+\frac{\beta}{2}M_\mathrm{H_2O}\right)+\left(\alpha+\frac{\beta}{4}-\frac{\gamma}{2}\right)\left(3.76\varphi_0 M_\mathrm{N_2}+\left(\varphi_0-\frac{1}{1-R_\mathrm{EGR}}\right)M_\mathrm{O_2}\right)}$$

Nomenclature

C_p – specific heat coefficient, [Jkg^{-1}K^{-1}]
D_h – hydraulic diameter of the pipe, [m]
f – friction factor
k – turbulent kinetic energy, [m^{2}s^{-2}]
L – length of the pipe, [m]
M_i – molar mass of species i, [kgmole^{-1}]
$\dot{m}$ – mass-flow rate, [kgs^{-1}]
n – number of tubes
P – pressure, [Pa]
P_o – operating pressure, [Pa]
Pr – Prandtl number ($=\mu C_p/\lambda$)
Pr$_\mathrm{t}$ – turbulent Prandtl number
R – shell outside radius, [m]
R$_\mathrm{gas}$ – universal constant of gas, [JK^{-1}mole^{-1}]
r – tube radius, [m]
S – strain rate, [s^{-1}]
T – temperature, [K]
U – tmean velocity in the tube, [ms^{-1}]
u – fluid velocity, [ms^{-1}]
Y_i – mass fraction of species i

Greek symbols

ε – turbulent energy dissipation, [m^{2}s^{-3}]
λ – conductivity coefficient, [Wm^{-1}K^{-1}]
μ – dynamic viscosity, [Pa·s]
μ_t – turbulent dynamic viscosity, [Pa·s]
ν – kinematic viscosity, [m^{2}s^{-1}]
ν_t – turbulent kinematic viscosity, [m^{2}s^{-1}]
ξ – cooling efficiency
ρ – fluid density, [kgm^{-1}]

σ_k – turbulent Prandtl number for k
σ_ε – turbulent Prandtl number for ε
φ_0 – excess-air ratio

Subscripts

i – inlet
o – outlet
g – gas
w – water

References

[1] Heywood, J. B., *Internal Combustion Engine Fundamentals*, McGraw-Hill, Inc., New York, USA, 1988
[2] Zheng, M., *et al.*, Diesel Engine Exhaust Gas Recirculation – A Review on Advanced and Novel Concept, *Energy Conversion and Management*, *45* (2004), 6, pp. 883-900
[3] Pierpont, D. A., *et al.*, Reducing Particulate and NO_x Using Multiple Injections and EGR in a D. I. Diesel, SAE technical paper 950217, 1995
[4] Charnay, L., *et al.*, CFD Optimization of an EGR Cooler for Heavy-Duty Diesel Engines, SAE technical paper, 2001-01-1755, 2001
[5] Park, S., *et al.*, Heat Exchange Efficiency Characteristics of EGR Cooler with Stack-Type or Shell and Tube-Type, SAE technical paper, 2007-01-3446, 2007
[6] Master, B. I., *et al*, Fouling Mitigation Using Helixchanger Heat Exchangers: *Proceedings,* The ECI Conference on Heat Exchanger Fouling and Cleaning, Santa Fe, N. Mex., USA, 2003, pp. 317-322
[7] Sunil, S. S., *et al*, Performance Improvement in Single Phase Tubular Heat Exchanger Using Continuous Helical Baffles, *International Journal of Engineering Research and Applications*, *2* (2012), 1, pp. 1141-1149
[8] Huang, Y. Q., *et al.*, Numerical Simulation and Optimization Design of the EGR Cooler in Vehicle, *Journal of Zhejiang University Science*, *9* (2008), 9, pp. 1270-1276
[9] Park, S., *et al.*, Effects of the Internal Shape of EGR Cooler on Heat Exchanger Efficiencies, SAE technical paper, 2007-01-1252, 2007
[10] ***, ANSYS Inc. Fluent User Guide and Fluent Theory Guide, Version 13.0, 2010
[11] Yaws, C. L., *Transport Properties of Chemicals and Hydrocarbons*, 1st ed., William Andrew Inc., Amsterdam, The Netherlands, 2009
[12] Kee, R. J., *et al.*, The CHEMKIN Thermodynamic Database, Technical Report Sandia National Laboratories, SAND87-8215, Albuquerque, N. Mex., USA, 1987
http://www.detchem.com/mechanisms/04_CH4_H2O_O2_Rh_Thormann2009td_CH4_H2O_O2_Rh_2009
[13] Asad, U., Zheng, M., Exhaust Gas Recirculation for Advanced Diesel Combustion Cycles, *Applied Energy*, *123* (2014), C, pp. 242-252
[14] Incropera, F. P., *et al.*, *Fundamentals of Heat and Mass Transfer*, John Wiley and Sons, Inc., New York, USA, 2007
[15] Purandarea, P. S., *et al.*, Experimental Investigation on Heat Transfer and Pressure Drop of Conical Coil Heat Exchanger with Parameters Tube Diameter, Fluid Flow Rates and Cone Angle, *Thermal Science*, *First Issue 00*, (2014), pp. 137-137, 2014
[16] Karuppa Raj, R. T., Ganne, S., Shell Side Numerical Analysis of a Shell and Tube Heat Exchanger Considering the Effects of Baffle Inclination Angle on Fluid Flow, *Thermal Science*, *16*, (2012), 4, pp. 1165-1174, 2012
[17] Kalaiselvam, S., *et al.,* Study of Heat Transfer and Pressure Drop Characteristics of Air Heat Exchanger Using PCM for Free Cooling Applications, *Thermal Science*, *20* (2016), 5, pp. 1543-1554
[18] Zimparov, V. D*., et al.,* Performance Evaluation of Tube-in-Tube Heat Exchangers with Heat Transfer Enhancement in the Annulus, *Thermal Science*, *10*, (2006), Issue 1, pp. 0354-9836

Paper submitted: August 30, 2016
Paper revised: December 14, 2016
Paper accepted: December 25, 2016

© 2018 Society of Thermal Engineers of Serbia
Published by the Vinča Institute of Nuclear Sciences, Belgrade, Serbia.
This is an open access article distributed under the CC BY-NC-ND 4.0 terms and conditions